A Miniaturized Low Power Biomedical Sensor Node for Clinical Research and Long Term Monitoring of Cardiovascular Signals

Jarno Tuominen*, Eero Lehtonen*, Mojtaba Jafari Tadi*‡, Juho Koskinen*, Mikko Pänkäälä* and Tero Koivisto*
* Technology Research Center, University of Turku, Finland. E-mail: jmtuom@utu.fi
‡Department of Cardiology and Cardiovascular Medicine, University of Turku, Finland

***Abstract*—We present a low power, miniaturized biomedical sensor node featuring electro-, seismo- and gyrocardiography. Measurement session can be set up and controlled over Bluetooth Low Energy interface. Acquired raw or preprocessed sensor data can be stored locally to the microSD memory card. To the best of the authors' knowledge, the presented device is the smallest reported to enable heart monitoring from the electrical and mechanical (with six degrees of freedom) viewpoint. The average power consumption of the device is less than 15mW, enabling continuous acquisition of high quality data of more than 60 hours with the used 250mAh Lithium-Polymer battery.**

I. Introduction

Today, the heart's activity can be investigated and measured by several methods, of which the most common are electrocardiography (ECG), echocardiography, phonocardiography, and photoplethysmography (PPG). In addition to these, in ballistocardiography (BCG) and in seismocardiography (SCG), inertial sensors are used to measure body movements and local chest vibrations resulting from the mechanical activity of the heart and from the blood ejection [1]. Advances in the MEMS-technology have made it possible to develop miniature low-power sensor nodes for unobtrusive monitoring, where SCG measurements are performed by attaching the sensor for example to the skin of the chest by adhesive. State-of-the art examples of such wearable devices are reported in [2], [3], [4]. MEMS-based BCG and SCG devices enable inexpensive access to mechanical cardiac monitoring, which has been used for example in atrial fibrillation detection [5], in monitoring the hemodynamics of heart failure patients [3], in determining quiescent phases in cardiac cycles for nuclear imaging [6], and in detecting myocardial infarction [7].

In addition to accelerometer-based SCG, it has been recently shown [8], [9] that gyroscope-based heart monitoring — here called *gyrocardiography (GCG)* — yields useful information for analyzing the underlying source of the motion of the sensor node: the movements of the heart, and blood ejection.

In order to facilitate further research in electromechanical cardiography and long-term monitoring of heart diseases, we present in this work a sensor node that offers simultaneous recording of 3-axis SCG, 3-axis GCG, and up to 5-lead ECG. The presented device is the smallest reported to contain both ECG and a 3-axis SCG, and the first that has been shown to reliably record GCG; inertial sensors in the available commercial products [10], [11] have been so far used to monitor large-scale body kinematics.

This work was funded by Tekes (40092/14) and the Academy of Finland (277383).

II. System architecture and specifications

A. System requirements

The device was designed to fulfill the following requirements:

- Length of the measurement session varies from minutes to days. Power consumption must be low enough for several days of continuous battery-operated measurements.
- Wearable and small enough to be used during daily activities.
- Can be operated by the patient at home, by hospital staff and by research scientists. The latter requires flexibility over sensor configurations and other system settings.
- Sample rate can vary between sensors or channels within a sensor, while maintaining the timebase in the data.
- Data acquisition does not degrade the accuracy of sensor subsystem.
- Multi-modal, support for simultaneous usage of multiple sensors and interface for external, wired sensors.
- Reliable and fault-tolerant operation to minimize data loss in case of error conditions. No missed samples are allowed in any of the sensors under normal conditions. Missed samples must be detected and indicated in the acquired data so that time base can be restored.
- Battery level is provided to the terminal and battery run-out is handled without data loss.

In accordance to the above requirements, the specifications of the presented sensor node are listed in Table I.

B. Hardware architecture

A simplified HW architecture of the device is shown in Fig. 1, while the PCB and designed mechanics are presented in Figs. 2 and 3. The HW architecture consists of the following blocks:

1) Microcontroller (μC) and BLE: The device is built around Nordic Semiconductor nRF51822, a 32-bit ARM Cortex M0-based μC with BLE radio. The CPU core runs at 16MHz offering 32kB SRAM and 256kB flash. Sensors are connected to μC with SPI-buses, SPI1 and SPI2, both running

TABLE I
DEVICE SPECIFICATIONS. SAMPLE RATES OF SENSORS REPRESENT OUR TYPICAL USE CASE.

Parameter	Value
Dimensions (l x w x h), in mm	46 x 27 x 5.7 (PCB only)
(see Fig. 3)	50 x 32 x 11.9 (with mechanics)
Accel. sample rate, BW, noise	200Hz, 80Hz, 1.6mg_{rms}
Gyro sample rate, BW, noise	200Hz, 74.6Hz, 1.5m°/s_{rms}
ECG leads	up to 5
ECG sample rate, BW, noise	267Hz, 55Hz, 1.18μV_{rms}
Battery, battery life	250mAh LiPo, >60 hours
Data storage capacity	max 32GB
Power consumption, avg	14.5 mW, w/gyro, acc., 3-lead ECG acquisition to μSDCard

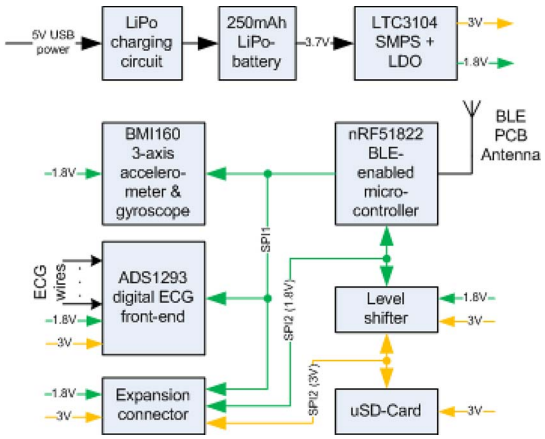

Fig. 1. System block diagram

at 4MHz. SPI1 is available only at 1.8V logical voltage levels, whereas SPI2 is available also at 3V via a two-way level shifter (TI TXS0108E). The level shifter is used also for control signals between the μC and 3V peripheral components.

The BLE radio antenna is designed on PCB and matched to RF output stage with a single-chip balun with harmonic filter.

2) Sensors subsystem: Bosch Sensortec BMI160 Inertial Measurement Unit (IMU) offers a 3-axis accelerometer and gyroscope in a single package. BMI160 has 1kB built-in FIFO

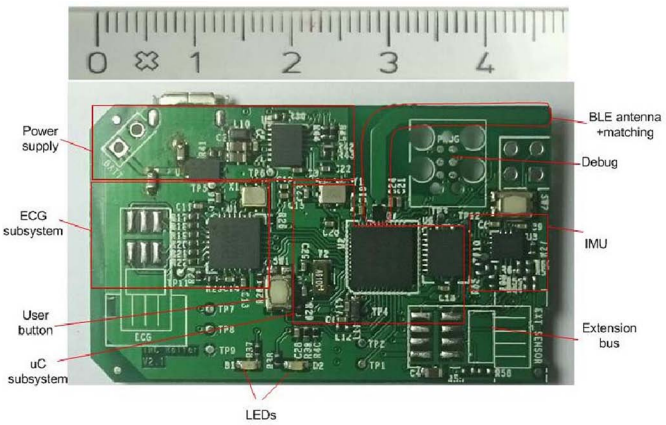

Fig. 2. PCB of the sensor node

with a programmable watermark level for interrupt generation, making it well-suited for an event-driven low power sensor node. BMI160 offers a rich set of configurable filters and signal processing features for interrupt generation, for example functions for detecting free-fall, "orientation" and high-G events.

Texas Instruments ADS1293 is the analog front-end for the ECG, up to 5 leads. ADS1293 provides data ready interrupt, which is routed to μC, as well as alarm signals indicating improper operating conditions.

3) Power supply and power domains: The design has two power domains: 3V is regulated from a 3.7V Lithium-Polymer (LiPo) battery using a switched mode power supply (SMPS), while 1.8V is regulated from 3V SMPS output using a linear low drop-out (LDO) regulator. Micro-USB is used as a charging connector and LiPo charging circuitry is included. Voltage regulators for both power domains are packed in a single IC (Linear Technology LTC3104). The maximum load current in 1.8V domain consists of CPU load ($\approx$ 2mA), sensors load ($\approx$ 1mA) and BLE radio load ($\approx$ 10mA peak). The LDO in LTC3104 is rated at 10mA continuous current, with 20mA current limit. The maximum peak load of 3V, up to 100mA, is caused by microSD card (μSDC). Therefore, 3V is regulated using the SMPS (rated at 300mA) and 1.8 V using the LDO.

LTC3104's SMPS can reach up to 95% efficiency with higher load currents. With the presented device, problems arise with the combination of low average load and high peaks, caused by the BLE and μSDC operations. The no-load input current of LTC3104 is $\approx$ 2.3mA with 3.7V V_{BAT}. This can be reduced by letting SMPS switch automatically between low-noise and burst modes, based on the output load. In burst mode, SMPS efficiency is $\approx$ 90% even at light loads. The drawback of using SMPS in burst mode is higher voltage ripple. As can be seen in Fig. 5, such ripple is not visible in the acquired signals.

The μC, BMI160 and I/O of ADS1293 can run at 1.8V, whereas the μSDC and ADS1293 core functions require 3V. The sensor connected to expansion slot can operate either on 1.8V or 3V, having 1.8V or 3V I/O-levels. This mixture of operating voltages justifies the use of two power domains.

4) microSD memory card: The μSD card is connected to μC with a dedicated SPI bus (SPI2). Memory card write operations can take longer time than the sampling interval of the sensors. Write transactions are divided into 512-byte block transfers. While, in general, SPI bus sharing is possible, many memory cards do not allow it during multi-block write transactions. By bus separation, μC can perform sensor read operations on SPI1 in between 512-byte block transfers taking place on SPI2. This way SPI2 and memory card remain idle and undisturbed, and will continue transfer of the next block once sensor operations are completed on SPI1.

Write cycle to a flash memory in μSDC causes read and write-back of (at least) one erasable block, consuming fixed amount of energy. Typical size of erasable block is 64kB. Therefore, the more memory is available for buffering the data, the less often μC needs to write to the memory card.

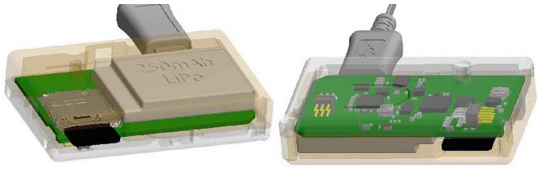

Fig. 3. Mechanics design for the device. Footprint is limited by the battery and the memory card slot, both placed on the bottom side. Height is limited by the battery (5.2mm), thickness of 4-layer PCB (1mm) and the button (1.7mm) on a top side of the PCB. The button (tactile switch) is in direct contact to the top cover of the mechanics. The plastic mechanics was 3D-printed in-house.

The chosen μC has only 32kB RAM, of which 12kB could be reserved for μSD FIFO. To prevent FIFO overflows, data write to memory card is triggered at 10kB data limit.

C. Embedded software operation

The software is strictly event-based, no real time operating system was used. The switching of operating states of the device, according to Fig. 4, are handled in the main context, based on the local button operations, timers and commands sent by the terminal over BLE. BLE commands are parsed in BLE event handlers and executed in main context, within the main state machine loop. Data acquisition from sensors is triggered by sensor-generated interrupts, asynchronous to μC clock. Time-critical functions, such as capturing ECG data from ADS1293, are executed in interrupt context. Less time-critical interrupts, such as BMI160's FIFO watermark interrupt can be handled in main context, as long as BMI160's FIFO is being read before overflow.

Sensor data is collected to circular buffers, and when enough data is available, a payload datagram with time stamp is created. Datagrams are collected to an output FIFO and further written to the μSD card in multiples of 512B blocks, when the FIFO is almost full. Each measurement session is created in its own directory, containing session logfile and several binary data files. The size of a single data file is limited to minimize the loss of data in case of system failure.

The data stored to μSD card is parsed with a MATLAB-script, which will read the session parameters, including patient information, session information and all the sensor parameters from the session log file. By using the sample rate of each sensor and the time stamp of each datagram, time base can be fully recovered. In case of data error or corrupted file, invalid data is skipped and rest of the data is still correctly aligned in time domain.

III. Measurements and Results

A. Power consumption measurements

The power consumption of the device depends on several parameters, such as the sample rate of sensors, the number of ECG leads, the type of the memory card, and the amount of usable buffer memory. The CPU sleeps most of the time, waking up only to serve interrupt requests from sensors and internal operations, such as battery monitoring, BLE communications and real time clock. The change in power consumption can be

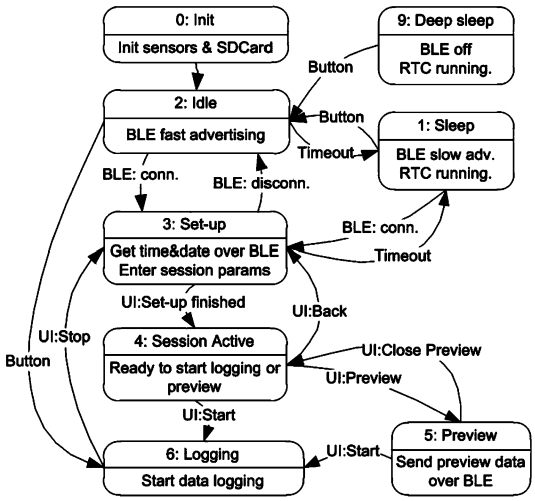

Fig. 4. State diagram of the sensor node

measured over a small (1Ω) shunt resistor, placed on negative lead of the battery. In this set-up, 1mA current causes 1mV voltage drop over the shunt and it is possible to see the profile of the total current, including power supply losses, by using an oscilloscope.

Our approach was to evaluate the cost of each device function – for example ECG – consisting of CPU activity, bus activity and sensor internal operations. By controlling the device states and sensor parameters over BLE, we can see the difference in total current, when a given function is turned on or off. The contribution of different functions to current consumption are listed in Table II. Sampling rate of gyroscope and accelerometer is 200Hz, ECG sampling at 267Hz. The column *Misc.* includes miscellaneous currents, mainly caused by usage of high-accuracy interrupt input pins within μC, which prevent shut-down of the 16MHz system clock during CPU idle periods. The penalty of this decreases as CPU activity increases.

B. Proof-of-Concept Measurements

The system functionality and acquired data quality was assessed by performing a series of measurements on several healthy test subjects in supine position, where the length of measurement sessions were in the range of minutes. The device was attached to test subjects sternum with adhesive tape. 4 snap-on ECG electrodes (RL,RA,LL,LA) were used to acquire 3 ECG leads (I,II and IV). Measured signal is shown in Fig. 5. The noise floor on the ECG signals is very low, with no visible noise coupled from the power supply, proving the SMPS can be used in burst mode. Signal from the MEMS sensor is clean and meets the expectations.

IV. Discussion and Conclusion

The power consumption is well aligned with the expectations. As the system is heavily duty-cycled and depends on the use case, focus should be put on minimizing constant currents. For the sensor subsystem not much can be done, but the

TABLE II
AVERAGE CURRENT AND POWER CONSUMPTION PER DEVICE FUNCTION, V_{BAT} = 3.7V

Configuration	μC+μSD activity	Lvl shift leakage	Acc.	Gyro	ECG	μSDCard leakage	SMPS losses	Misc.	Iavg	Pavg
Sleep, no μSDCard	0.01				0.08		0.01	(0.00)	0.10	0.37
Idle, μSDCard mounted	0.13	0.2			0.08	0.20	0.07	(0.00)	0.68	2.50
1ch ECG	0.23	0.2			0.28	0.20	0.19	0.81	1.91	7.07
Acc.	0.27	0.2	0.15		0.08	0.20	0.18	0.74	1.83	6.77
Gyro	0.28	0.2		0.68	0.08	0.20	0.25	0.78	2.47	9.14
3ch ECG	0.48	0.2			0.68	0.20	0.26	0.74	2.56	9.47
1ch. ECG, acc.	0.42	0.2	0.15		0.28	0.20	0.23	0.82	2.30	8.51
Acc.+ gyro	0.49	0.2	0.15	0.68	0.08	0.20	0.29	0.78	2.87	10.62
3ch. ECG, acc.+gyro	1.08	0.2	0.15	0.68	0.68	0.20	0.39	0.53	3.92	14.50

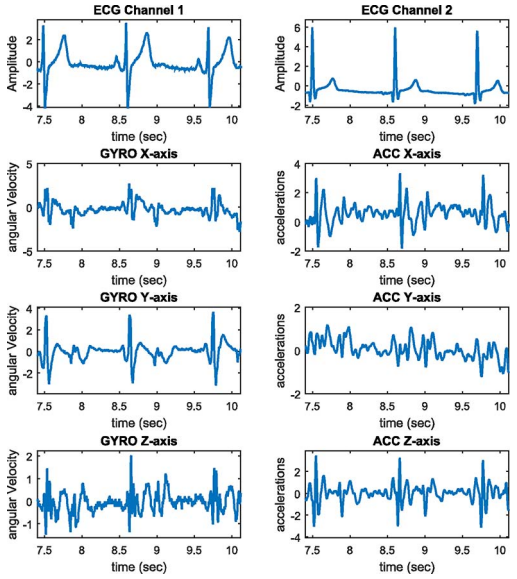

Fig. 5. Example results of concurrent ECG, SCG and GCG measurements, showing good quality on all measured channels.

active clock oscillator of the ECG is a bad choice, as it draws almost 1mA continuous current. A simple approach is to use a standard 4MHz SMD crystal, as is done with device used for the power measurements, but its size is rather large. A better silicon oscillator, such as LTC6907 by Linear Technology, would be better fit both in terms of size and power.

While the μSDC operations have highest peak current, low duty ratio makes its contribution relatively low. The duty ratio of SPI-buses could be improved further by introducing a faster CPU, preferably with a DMA controller. For example one could use Nordic Semiconductor nRF52-series, with 64MHz Cortex M4 core and a DMA support.

In order to decrease power consumption, the focus should put on the system level. One method is smart sample rate and power control of sensors. The motion artifacts are difficult to compensate from the MEMS data, suggesting that sensors should be set to lower sample rate during high-motion periods, and ECG could be shut down. BMI160 has "no motion"-interrupt, which can activate the system once conditions are feasible for data acquisition. Instead of storing raw data to the μSDC, only relevant signal features could be extracted and stored instead. This is an interesting research topic, as it requires balancing between the power used for computation and for data storage or transmission.

The measured signal quality is excellent, making this device a good fit for the intended purpose. The presented sensor node is smallest of its kind and the first to include inertial sensor of 6 axes of freedom, combined with ECG.

REFERENCES

[1] O. Inan, P.-F. Migeotte, K.-S. Park, M. Etemadi, K. Tavakolian, R. Casanella, J. Zanetti, J. Tank, I. Funtova, G. Prisk, and M. Di Rienzo, "Ballistocardiography and seismocardiography: A review of recent advances," *Biomedical and Health Informatics, IEEE Journal of*, vol. 19, pp. 1414–1427, July 2015.

[2] Y. Chuo, M. Marzencki, B. Hung, C. Jaggernauth, K. Tavakolian, P. Lin, and B. Kaminska, "Mechanically flexible wireless multisensor platform for human physical activity and vitals monitoring," *IEEE transactions on biomedical circuits and systems*, vol. 4, no. 5, pp. 281–294, 2010.

[3] M. Etemadi, O. T. Inan, J. A. Heller, S. Hersek, L. Klein, and S. Roy, "A wearable patch to enable long-term monitoring of environmental, activity and hemodynamics variables," *IEEE Transactions on Biomedical Circuits and Systems*, vol. 10, pp. 280–288, April 2016.

[4] P. Castiglioni, A. Faini, G. Parati, and M. Di Rienzo, "Wearable seismocardiography," in *2007 29th Annual International Conference of the IEEE Engineering in Medicine and Biology Society*, pp. 3954–3957, IEEE, 2007.

[5] C. Brüser, J. Diesel, M. Zink, S. Winter, P. Schauerte, and S. Leonhardt, "Automatic detection of atrial fibrillation in cardiac vibration signals," *Biomedical and Health Informatics, IEEE Journal of*, vol. 17, pp. 162–171, Jan 2013.

[6] M. J. Tadi, E. Lehtonen, J. Teuho, A. Saraste, M. Pänkäälä, M. Teräs, and T. Koivisto, "A miniaturized MEMS motion processing system for eliminating motion-related inaccuracies in PET imaging," in *Proceedings of Computing in Cardiology*, Sept 2016.

[7] T. Koivisto, O. Lahdenoja, T. Hurnanen, M. J. Tadi, E. Lehtonen, T. Vasankari, A. Saraste, T. Kiviniemi, J. Airaksinen, and M. Pänkäälä, "Detecting indications of acute myocardial infraction using smartphone only solution," in *European Congress on e-Cardiology & e-Health*, Oct 2016.

[8] P.-F. Migeotte, V. Mucci, Q. Delière, L. Lejeune, and P. van de Borne, "Multi-dimensional kineticardiography a new approach for wearable cardiac monitoring through body acceleration recordings," in *IFMBE Proceedings of the XIV Mediterranean Conference on Medical and Biological Engineering and Computing*, pp. 1125–1130, Sept 2016.

[9] M. J. Tadi, E. Lehtonen, M. Pänkäälä, A. Saraste, T. Vasankari, M. Teräs, and T. Koivisto, "Gyrocardiography: A new non-invasive approach in the study of mechanical motions of the heart. concept, method and initial observations," in *2016 38th Annual International Conference of the IEEE Engineering in Medicine and Biology Society (EMBC)*, pp. 2034–2037, Aug 2016.

[10] shimmer™, ECG & EMG Unit, http://www.shimmersensing.com/.

[11] MC10®, BioStamp Research Connect™, https://www.mc10inc.com/our-products/biostamprc.